Scientific Documentation of Seatrack Web; physical processes, algorithms and references

Olof Liungman and Johan Mattsson

1 March 2011

1 Purpose

The purpose of this appendix is to present a scientific description of Seatrack Web HELCOM. It is intended to give an overview of the processes, algorithms and methods which Seatrack Web is based on. The documentation focuses on the oil drift model PADM (PArticle Dispersion Model), the program that performs the drift simulations requested by the user.

2 Fundamentals

2.1 System overview

The Seatrack Web system consists of three main parts: forcing in the form of forecasted flow and wind fields, an oil drift model and a graphical user interface. The oil drift model PADM has been jointly developed by the Swedish Meteorological and Hydrological Institute (SMHI) and the Danish Maritime Safety Administration (DAMSA). It is executed whenever a Seatrack Web user requests a simulation. The graphical user interface has been developed at SMHI and is based on open source GIS-server technology, i.e. the user interacts with georeferenced data in a map.

The area covered by the Seatrack Web HELCOM system is the Baltic Sea, the sounds between Sweden and Denmark, the Kattegat and the Skagerrak, and the North Sea to about longitude 3° east.

The forcing fields for Seatrack Web HELCOM are presently provided by the weather model HIRLAM and the ocean model HIROMB. These are run operationally and form the basis for weather and ocean forecasts at SMHI. For longer forecasts forcing fields from the European Centre for Medium-Range Weather Forecasts[1] replace those from HIRLAM.

---

[1] See ECMWF homepage

2.2 Conceptual model

The oil drift model PADM is a Lagrangian particle spreading model. This means that the substance or object being simulated is represented as a cloud of particles. The trajectory of each particle is calculated based on time- and space-varying flow fields.

At present it is assumed that the particles do not influence the flow field, i.e. a particle does not have any effect on the flow in which it is located.

Particles are affected by boundaries such as the coastline, the bottom or the surface. Particles cannot pass through a solid boundary but may either stick to a boundary or slip along it.

Each particle has a set of properties. Most important of these is of course its position. However, a particle can have a variety of additional properties depending on what substance or object it represents, e.g. mass, volume, size, chemical properties, density, etc. These can be constants or vary with time, location, temperature, etc.

In the current version of Seatrack Web HELCOM, algorithms have been implemented for the following substances:

- oils,

- tar balls,

- floating objects or algae, and

- passive tracers.

Tar balls are currently treated as passive floating objects.

The processes that as of today have been included in PADM can be divided into two main sections: spreading, which includes all processes related to the movement of the particles, and weathering of oil.

2.3 Time and space discretization

Before continuing we must describe how the real world is represented in the model. To begin, it is assumed that the flow field is defined in a discrete, structured grid of six-sided cells at discrete times (see Figure 1). The grid discretization is assumed to be staggered, i.e. the flow velocities are located on the faces of each grid cell. Within a given grid cell the flow field is determined by the velocities on the six faces, with the assumption that u, the velocity component in the x-direction, only varies in the x-direction, v, the velocity in the y-direction, only varies in the y-direction, and w, the velocity component in the z-direction, only varies in the z-direction. In other words, the perpendicular velocity component on a particular face is constant over that face.
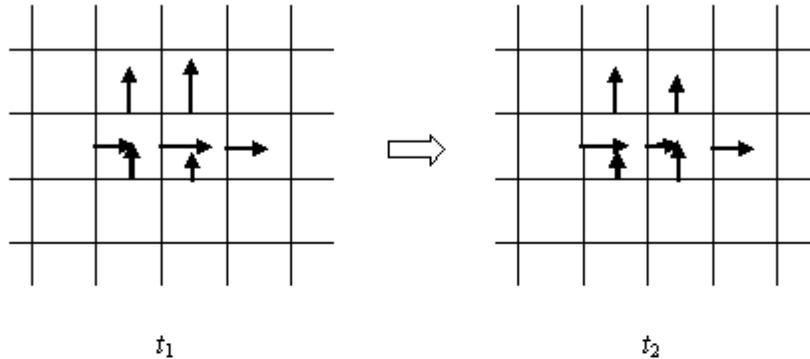
Figure 1: A schematic 2-D view of the internal grid, showing the space and time discretization. For clarity only a few flow vectors are shown.

As time progresses beyond the current interval, the flow field changes abruptly and is then constant in time for the following time interval, and so on.

The model representation implies that for a given time interval the flow parameters at each location in the grid are constant in time, but may vary spatially. The spatial variation is of course limited by the grid resolution and the temporal variation by the time step. This means that we have two fundamental time scales: the time it takes a particle to reach the next grid cell T_u and the time step between successive flow fields T_t.

Note that the grid described above is a strictly internal representation. Thus, when talking about x, y and z it is the internal coordinate directions that are referred to. All positions and velocities are referenced in a system based on the indices of the grid cells and the local position within a given cell (see Figure 2)[2]. So-called transformation functions, which handle the conversions between real world coordinates and the internal representation in PADM, need to be specified.

In Seatrack Web HELCOM the internal PADM grid is mapped onto the HI-ROMB grid, an orthogonal, structured grid in spherical coordinates. In HI-ROMB the x-direction runs from west to east (longitude), the y-direction from south to north (latitude) and the z-direction points upwards (inverted depth).

The bottom boundary in PADM is defined by the bottom in the HIROMB computational grid. Thus, the bottom at a particular location is represented by the horizontal face of the lowermost grid cell at that location, which in turn is defined by the HIROMB bathymetry. Because HIROMB uses a grid with constant levels in the vertical (z-level) a sloping bottom will be represented by

---

[2]The cell indexing begins in the bottom lower left cell (1,1,1) and increases to the right (x-index), upwards (y-index) and towards the surface (z-index).
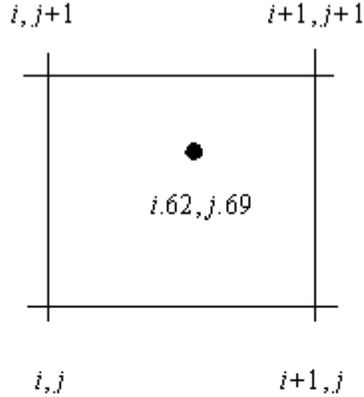
3

Figure 2: A 2-D schematic showing how internal positions are defined in the grid. The point indicated is located in cell (i, j) and its local position within that cell is (0.62, 0.69), where the local origin is located in the corner node designated (i, j) and the extent of the cell is unity in all directions.

a stairway shape. Hence a particle reaching the bottom may interact with a horizontal or a vertical face of a grid cell (see Figure 3).

The surface boundary is simply the upper face of the uppermost grid cells. Varying sea levels are not taken into account in the particle spreading calculations.

The lateral boundaries at the surface, i.e. the coastline, are not defined by the PADM grid. Instead, a coastline digitised from available charts is used. Thus the coastline is described in greater detail than that allowed by the horizontal resolution of the grid. The coastline consists of a large number of line segments. Each line segment actually constitutes the upper edge of a vertical face which stretches down to the bottom at the grid location where the coastline segment is located (see figure 4).

Because PADM is not restricted to the resolution and boundaries set by the HIROMB grid, there may be grid cells which are considered dry in HIROMB but part of which are considered wet by PADM, i.e. if the coastline runs through a HIROMB cell which has been defined as dry. In these cells, HIROMB obviously cannot provide any current velocities or scalar properties such as salinity or temperature. To provide a better approximation of the advective current field in these cells a velocity directly proportional to the wind velocity is inserted into the forcing fields. Presently the constant of proportionality is 0.01, i.e. 1 %, based on comparisons between the surface current in HIROMB and wind speeds. Scalar fields such as salinity and temperature are extrapolated from the nearest wet HIROMB cells.
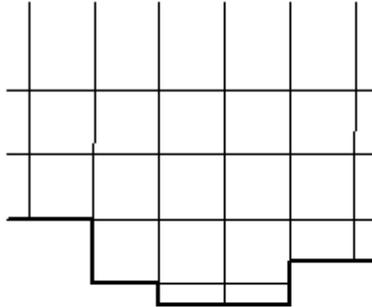
4

Figure 3: A 2-D vertical section through the HIROMB grid showing the staircase approximation of the bottom (thick line).

3   The effect of ice

Ice is not explicitly modelled as a moving physical boundary in the current version of Seatrack Web. Furthermore, the model focuses on the effect of ice on oil already on the surface, and thus neglects transport or storage of oil under ice. Because a large relative velocity difference between the sea and the drifting ice is required to push oil reaching the ice edge down below the ice, this process is also neglected. Instead, simple parametrisations are used to simulate the effect of ice on the particles at the surface. The parametrisations have been determined from a compilation of the available literature on the effect of ice on oil spilled at sea [1, 2, 3, 5, 9, 8, 12, 18, 22, 24, 25, 27, 28, 29]. The parametrisations are based on the basic concept that ice will reduce the intensity of the wave field, thereby reducing the Stokes's drift and the dispersion, and reduce the available surface area, hence increasing the oil thickness and thus affecting the gravity-induced spreading and weathering of oil.

The presence of ice influences the hydrodynamic current field (see section 4.1), the surface Stokes's drift velocity (see section 4.2), the horizontal gravity-induced spreading of oil (see section 4.3), the dispersion of oil (see section 4.4) and the weathering of oil (see section 5). When the ice concentration exceeds a certain limit, the ice drift velocity will determine the particle velocity at the surface rather than the hydrodynamic current field. For the other three processes the ice enters as a correction coefficient which is a simple function of the ice concentration. The required inputs are hence the ice concentration and the ice drift velocity. In Seatrack Web HELCOM this input is generated by the ice model in HIROMB.
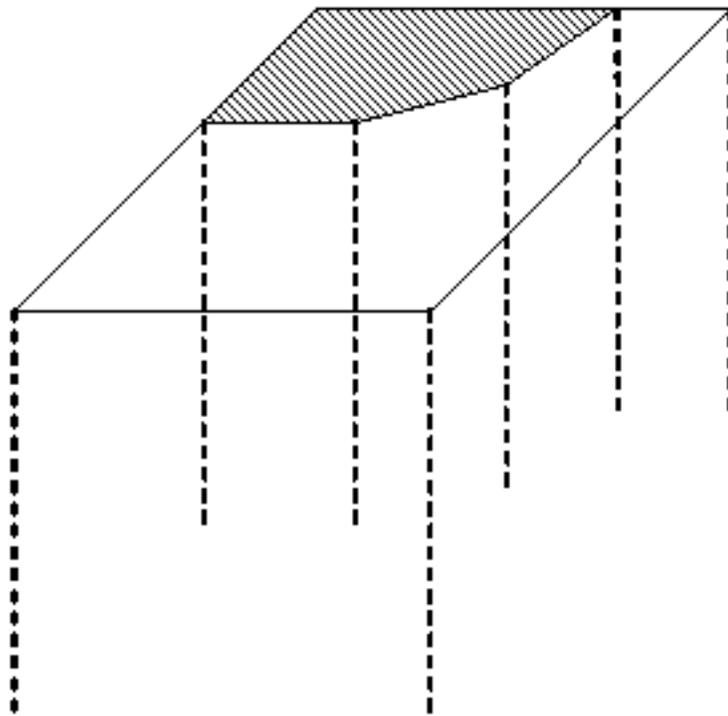
Figure 4: A schematic showing how a detailed coastline consisting of three line segments intersects a grid cell (the shaded area is considered to be up on land). Note also how the line segments extend down into the water column all the way to the local bottom, forming vertical surfaces that are treated as bottom areas.

6

4 Spreading

Spreading is here defined as the movement of particles from their point of origin. In PADM a number of different processes can generate velocities that cause spreading. The net velocity is calculated as the sum of these different velocities. The processes currently implemented are:

- the current (generated by the hydrodynamic model),

- unresolved wave-induced Stokes's drift,

- horizontal gravity-induced radial spreading of a surface oil slick,

- wave-induced dispersion from the surface into the water column,

- isotropic turbulent mixing in the water column, and

- sinking or rising due to buoyancy differences.

In addition, the spreading is influenced by the interaction of particles with physical boundaries. Note that only the hydrodynamic current field includes the velocity gradient, whereas the remaining velocities are only given at a point, namely the position of the particle in question (see section 4.1). More detailed descriptions of each process and how they are modelled in PADM are given below.

When running a simulation in PADM one must first specify the particles initial, or outlet, positions. For example, in the case of oil this can be the actual source of the oil spill or the location where an oil spill has been discovered. Various alternatives are available in Seatrack Web HELCOM:

1. all particles start at a single position,

2. all particles are evenly distributed along a line, or

3. all particles are evenly distributed over a triangular or quadrilateral area.

In addition, particles can be released:

A. all at the same time (instantaneous discharge), or

B. in sequence over a given period of time (continuous discharge of specified duration).

A combination of release alternatives 2 and B yields a situation where particles are released in sequence along a line. If the duration of the discharge is set to the time it takes for a vessel to move from the start point of the line to the end point, this mimics a continuous discharge from a moving vessel.

Finally, the initial position may be

7

1. on the surface (default situation), or

2. below the surface at a given depth (e.g. oil leak from a sunken vessel).

In the current version, particles whose initial positions are on land or under the bottom (if, e.g., the outlet area intersects with the coastline) are not included in the calculation.

It should also be noted that the current algorithm for distributing particles evenly over an outlet area is approximate and may in certain cases produce corners in the outlet area without particles or a smaller number of particles than requested by the user.

4.1 Advection algorithm

This section deals with the fundamental algorithm of a Lagrangian particle tracking model, namely the passive advection of particles in a flow field.

4.1.1 Assumptions

Firstly, the spreading algorithm assumes that the particles can be treated as infinitesimal, i.e. they have no extent, no inertia and do not interact. They simply follow the streamlines of the flow. However, the net velocity field that constitutes the input to the algorithm is the sum of the hydrodynamic current field and point velocities that may depend on particle properties such as diameter or interaction between particles (see list under section 4).

Secondly, PADM deals primarily with submerged particles. This means that it is the hydrodynamic current field which moves the particles, in addition to the particle-specific point velocities. The current field, in turn, is a result of the combined effect of wind, tides and barotropic and baroclinic pressure gradients. However, for floating objects it is possible to add a particle velocity due to direct wind drag, expressed as a percentage of the forcing wind velocity. This would be appropriate if the object represented by the particles is buoyant and floats partially out of the water, e.g. a life raft.

4.1.2 Theory

Passive advection in one dimension of a Lagrangian tracer is described by the equation

$$\frac{d\boldsymbol{x}_P}{dt} = \boldsymbol{v}\left(\boldsymbol{x}_p\left(t\right)\right) \tag{1}$$

Here, $\boldsymbol{x}_P(t) = (x_P(t), y_P(t), z_P(t))$ is the particle position at time t and $\boldsymbol{v}(\boldsymbol{x}_P(t))$ is the corresponding velocity vector determined by the flow field. For simplicity, we will henceforth only consider the x-component, i.e.

$$\frac{dx_P}{dt} = u(\boldsymbol{x}_P(t)) \tag{2}$$

If we consider a particle during a single time step and within a single grid cell then the assumptions presented in section 2.3 regarding the time and space discretization imply that the flow component u can be described as a linear function of x_P only:

$$u = u_0 + (x_P - x_0)\frac{du}{dx} \tag{3}$$

where $u_0 = u(x_0)$, $x_0 = x_P(t_0)$ and $\frac{du}{dx}$ is constant[3]. Thus,

$$\frac{dx_P}{dt} = u_0 + (x_P - x_0)\frac{du}{dx} \tag{4}$$

Integrating this equation with respect to t yields, after some mathematical manipulation,

$$x_P(t) = \frac{u_0}{\frac{du}{dx}}\left(e^{\frac{du}{dx}(t-t_0)} - 1\right) + x_0 \tag{5}$$

See, e.g., [26] for a detailed derivation. Now, if $\Delta x_P = x_P(t) - x_0$, $\Delta t = t - t_0$ and $\frac{du}{dx} = \frac{\Delta u}{\Delta x}$, where Δx is the length of the grid cell in the x-direction and $\Delta u = u_r - u_l$ is the velocity difference between the right and left faces, then

$$\Delta x_P = \frac{u_0 \Delta x}{\Delta u}\left(e^{\frac{\Delta t \Delta u}{\Delta x}} - 1\right) \tag{6}$$

In case of zero velocity gradient ($\Delta u = 0$), the trivial solution is

$$\Delta x_P = u_0 \Delta t \tag{7}$$

The equations for the change in particle position in the y- and z-direction are identical, with x replaced by y or z and u with v or w, respectively.

Within the restrictions of the underlying assumptions about the discretization of space and time the equations for the change in the particle position are exact. In other words, the equations describe the streamline along which a particle will move (i.e. the particle's trajectory) as long as $\Delta t \leq \min(T_u, T_t)$. Furthermore,

---

[3]Note that u_0 is the sum of velocities calculated by the hydrodynamic model and the point velocities produced by different unresolved or particle dependant processes, whereas $\frac{du}{dx}$ is only given by the hydrodynamic flow field.

we can solve the equations analytically for t and determine when the particle reaches a certain position, such as the face of a grid cell.

When the particle reaches the face of a grid cell and enters a new grid cell, the parameters in the equations change. The same is true when when the forcing flow field is updated.

4.1.3   Implementation details

If the user has specified an extra wind factor and the particles represent a floating object, the specified fraction of the wind speed is simply added component-wise to the horizontal flow velocities affecting the particles.

For two-dimensional advection, i.e., when considering a floating object or an object that maintains a given depth, the vertical component of the particle velocity is set to zero.

In the case of ice, the hydrodynamic surface current field is modified. For high ice concentrations C_{ice} and for particles on the surface only, the hydrodynamic current velocity is set equal to the ice drift velocity $\boldsymbol{v}_{ice}$, i.e. for the x-component of the surface velocity (and similarly for the y-component)

$$u\left(z=0\right) = \begin{cases} u_{ice} & C_{ice} > 0.7 \\ u\left(z=0\right) & C_{ice} \leq 0.7 \end{cases} \tag{8}$$

4.2   Stokes's drift

To provide a realistic spreading it is necessary to account for the Stokes's drift. This is handled by calculating the Stokes's drift velocity for each particle in the oil drift model. This velocity is added to the horizontal surface current in the hydrodynamic forcing fields. In the present version of Seatrack Web the Stokes's drift speed (u_s, v_s) is calculated as a sum over N and M discrete frequencies f_i and directions θ_j, respectively, according to

$$\begin{cases} u_s = r_{ice} \sum_i^N \sum_j^M \Delta a_{i,j}^2 \, k_i \omega_i e^{2k_i z} \, cos(\theta_j) \\ v_s = r_{ice} \sum_i^N \sum_j^M \Delta a_{i,j}^2 \, k_i \omega_i e^{2k_i z} \, sin(\theta_j) \end{cases} \tag{9}$$

Here, $\omega_i = 2\pi f_i$ is the angular frequency, k_i the wave number and z the vertical coordinate (zero at the surface, positive upwards). The dispersion relation, assuming deep water, yields $k_i = \omega_i^2/g$ and the binned amplitude squared is given by

$$\Delta a_{i,j}^2 = 2S(f_i, \theta_j)\Delta f_i \Delta \theta_j$$

$S(f, \theta)$ is the two-dimensional wave energy spectrum. $\triangle f_i = \varepsilon f_i$, where $\varepsilon = 0.1$ and $f_{i+1} = f_i + \triangle f_i$. The frequency f_i ranges from $f_1 = 0.04$ to $f_N = (1+\varepsilon)^{N-1} f_1 \approx 5.17$ Hz with $N = 52$ frequency bins. There are 25 angular bins, with $\triangle \theta_j = 2\pi/25$. The Stokes's drift velocity is modified by the presence of ice by multiplying with the factor r_{ice}, where

$$r_{ice} = \begin{cases} 0 & C_{ice} > 0.7 \\ 1 - \frac{C_{ice}}{0.7} & C_{ice} \leq 0.7 \end{cases} \tag{10}$$

The reason for this is that the presence of ice is expected to decrease the intensity of the wave field (see 3).

Currently Seatrack Web HELCOM does not import wave spectra from an operational wave forecast model. Instead, a parameterised spectrum is used, at present the Donelan-Banner spectrum ([10]) for fetch-limited growth. The Donelan-Banner spectrum has the form

$$S(f, \theta) = \frac{\alpha_d g^2}{(2\pi)^4 f^5} \frac{f}{f_p} exp(-(\frac{f_p}{f})^4) \gamma_d^\Gamma H(f, \theta) \tag{11}$$

where

$$\Gamma = exp(\frac{-(f - f_p)^2}{2\sigma_d^3 f_p^2}) \tag{12}$$

with

$$\alpha_d = 0.006 \left(\frac{W}{c_p}\right)^{0.55} \; for \; 0.83 < \frac{W}{c_p} < 5 \tag{13}$$

$$\gamma_d = \begin{cases} 1.7 & 0.83 < \frac{W}{c_p} < 1 \\ 1.7 + 6.0 \log_{10}(\frac{W}{c_p}) & 1 \leq \frac{W}{c_p} < 5 \end{cases} \tag{14}$$

$$\sigma_d = 0.08 \left(1 + \frac{4}{(\frac{W}{c_p})^3}\right) \; for \; 0.83 < \frac{W}{c_p} < 5 \tag{15}$$

Here, f_p is the peak frequency, $c_p = g/(2\pi f_p)$ and W is the 10 meter height wind speed.

The directional spread is described by the term

$$H(f, \theta) = \frac{1}{2} \beta \, sech^2(\beta(\theta - \theta_w)) \tag{16}$$

where θ_w is the wind-sea direction. Donelan et al. ([10]) determined β by empirical fitting,

$$\beta = \begin{cases} 2.61\,(\frac{f}{f_p})^{1.3} & 056 < \frac{f}{f_p} < 0.95 \\ 2.28\,(\frac{f}{f_p})^{-1.3} & 0.95 \le \frac{f}{f_p} < 1.6 \end{cases} \tag{17}$$

Banner ([4]), based on experiments for $f/f_p > 1.6$, found

$$\beta = exp_{10}\left(-0.4 + 0.8393\,exp(-0.567\,ln((\frac{f}{f_p})^2))\right) \ \ for \ \frac{f}{f_p} \ge 1.6 \tag{18}$$

Kahma and Calkoen ([15]) found from a composite of several experiments with fetch limited growth that there is a general relation between the fetch F and the wave age c_p/W over deep water, which they determined as

$$\frac{W}{c_p} = 13.7(\frac{W^2}{gF})^{0.27} \tag{19}$$

which gives

$$f_p = \frac{g}{2\pi W}\frac{W}{c_p} = \frac{13.7\,g}{2\pi W}(\frac{W^2}{gF})^{0.27} \tag{20}$$

As a pragmatic approach for fully developed sea or very young sea (e.g., close to the shore), i.e. for conditions outside the validity range $0.83 < \frac{W}{c_p} < 5$, $\frac{W}{c_p}$ is set to the constant end point value of the range and the peak frequency for $g = 9.81$ becomes

$$f_p = \begin{cases} 1.30/W & , W^2 \le F/3300 \ \ (\frac{W}{c_p} = 0.83) \\ 7.81/W & , W^2 \ge F/4.26 \ \ (\frac{W}{c_p} = 5) \end{cases} \tag{21}$$

The fetch F in Seatrack Web is calculated as the distance from the nearest shoreline to the current computational cell for a fixed number of different directions. Presently eight directions evenly distributed around the compass are used. The fetch is limited to a minimum value equal to the horizontal resolution and a maximum value of 270 nautical miles. The maximum value is equivalent to the required fetch to reach fully developed sea at a wind speed of 12 m/s.

4.3   Horizontal surface spreading

We differentiate between turbulent mixing in the water column and horizontal spreading near the surface. This division is particularly useful for oil, which in

12

general behaves as an integrated slick on the surface but as individual droplets in the water column. Horizontal spreading is the result of horizontal current shears (at various spatial and temporal scales) and, in the case of oil, self-induced spreading in a balance between viscous and gravitational forces.

Currently, only two sub-grid scale horizontal spreading processes are implemented. These are the horizontal components of small-scale isotropic turbulence (see section 4.5 Mixing) and the gravity-induced radial spreading of an oil spill. The latter is primarily relevant during the early phase of an oil spill discharge.

Other sub-grid scale processes can of course be postulated. Variations on small temporal and spatial scales in both the current and wind field, e.g., eddies, Langmuir circulation, gusts, and so forth, which are not well represented in the forecasting models, will serve to spread a substance in water. Further development of Seatrack Web will attempt to include the effects of these processes. Note that one important spreading mechanism, the combined effect of vertical dispersion and vertical current shear, is included through the use of three-dimensional currents fields.

In the present version the gravity-induced horizontal spreading of oil is based on Fay's formula for the gravity-viscous spreading phase [17]:

$$A_{oil}\left(t\right) = 2.1\pi \left(\frac{V^2 g'_{oil}}{\sqrt{\mu/\rho}}\right)^{1/3} \sqrt{t} \tag{22}$$

Here, $A_{oil}\left(t\right)$ is the time-varying area of the oil slick, V is the spilled volume of oil, μ is the viscosity of water, ρ is the density of water and

$$g'_{oil} = g\frac{\rho - \rho_{oil}}{\rho}$$

is the buoyancy acceleration of oil with density ρ_{oil}. Adding a correction factor for for the oil viscosity μ_{oil} as well as the presence of ice yields the following modified formula [8]:

$$A_{oil}\left(t\right) = \left(\frac{\mu_{oil}}{\mu}\right)^{-0.15} \left(1 - C_{ice}\right) 2.1\pi \left(\frac{V^2 g'_{oil}}{\sqrt{\mu/\rho}}\right)^{1/3} \sqrt{t} \tag{23}$$

Since $-1/2 \times 1/3 \approx -0.15$, this is approximately equivalent to

$$A_{oil}\left(t\right) = \left(1 - C_{ice}\right) 2.1\pi \left(\frac{V^2 g'_{oil}}{\sqrt{\mu_{oil}/\rho}}\right)^{1/3} \sqrt{t} \tag{24}$$

In short, we replace the water viscosity by the viscosity of the oil [24].

In order to use equation 24 - which describes the evolution of a global property of an oil slick - to describe the spreading of individual particles that represent the oil slick, we first rewrite 24 in terms of the change in the oil slick's thickness h, using $V = hA_{oil}$:

$$\Delta h = h\Delta t \frac{1}{V}\frac{dV}{dt} - \Delta t \left(\frac{k_h^2 h^3}{2V^{2/3}}\right) \tag{25}$$

where

$$k_h = (1 - C_{ice})\, 2.1\pi \left(\frac{g'_{oil}}{\sqrt{\nu_{oil}\rho_{oil}/\rho}}\right)^{1/3} \tag{26}$$

This means that the slick thickness changes as a result of two processes: changes in the volume and gravitational spreading. The change in volume is both due to more oil being spilled and reduction in the volume due to weathering and can thus be written

$$\frac{dV}{dt} = \frac{dV_s}{dt} + \frac{dV_w}{dt} \tag{27}$$

where subscript s signifies increased spill volume and subscript w signifies weathering. Now, inserting 27 into 25 yields

$$\Delta h = h\Delta t \frac{1}{V}\frac{dV_s}{dt} - \Delta t \left(\frac{k_h^2 h^3}{2V^{2/3}}\right) + h\Delta t \frac{1}{V}\frac{dV_w}{dt} \tag{28}$$

Here, the first two terms on the right hand side represent changes in the global properties of the slick or particle cloud (Δh_{cloud}), whereas the third term represents weathering which is something that occurs for each particle individually (Δh_{part}). The change in volume due to weathering thus includes a summation over all particles. Finally, we can write the equation for the new oil slick thickness h_{new} after one time step Δt:

$$h_{new} = h + \Delta h = h + \Delta h_{cloud} + \Delta h_{part} \tag{29}$$

Equation 29 is used for each particle individually. Hence, the change in the oil thickness of each particle is determined both from the global change in volume, the global gravitational spreading and the change in each particle's volume due to weathering. Note that only particles on the surface are considered. The oil thickness has a lower bound set by the terminal thickness h_T. This is determined from the empirical formula (see [24])

$$h_T = 10^{-6} \times \frac{\mu_{oil}}{125} \tag{30}$$

14

In Seatrack Web, h_T is limited to a maximum value of 0.1 m. For particles that have been submerged a very simple model is used to determine the oil thickness at the surface; the thickness for these particles is set to the terminal thickness. Note that when calculating the global properties only particles who have not reached their terminal thickness are included.

The initial value of the thickness h_0 is determined as follows. For an instantaneous release, the initial thickness is set to the value at the transition between Fay's gravity-inertial phase and gravity-viscous phase, i.e. we are assuming the time until this transition to be short. Equating Fay's spreading formulae for the two phases at the time of transition and using $V = hA_{oil}$ yields

$$h_0 = \frac{V^{1/6}}{B_h} \tag{31}$$

where

$$B_h = 3.4\pi \left(\frac{g'_{oil}}{\left(\mu_{oil}/\rho\right)^2} \right)^{1/6} \tag{32}$$

For a continuous release, the initial thickness is chosen such that there is a balance between the increase due to the continuous spill and decrease due to spreading, that is

$$\Delta h = 0 \Rightarrow h_0 = \left(\frac{2\frac{dV_s}{dt}}{C_h^2 V^{1/3}} \right)^{1/2} \tag{33}$$

where

$$C_h = 2.1\pi \left(\frac{g'_{oil}}{\sqrt{\mu_{oil}/\rho}} \right)^{1/3} \tag{34}$$

Finally, to calculate the horizontal spreading of the particles representing the slick, we model each oil particle as a disc. Each particle disc has a time-varying thickness calculated according to equation 29. Using the volume of each particle we can then calculate the area and radius of each individual disc. Neglecting the fact that a cloud of non-overlapping discs will leave small gaps that are not covered, we assume that this cloud represents the extents of the oil slick if the discs are packed as closely as possible without overlapping. The purpose of the algorithm is thus to separate overlapping discs to accurately represent the extents of the slick. As the thickness of the discs decreases with time, the radii of the discs will increase (for the sake of argument neglecting volume changes due to weathering), they will be pushed apart and the slick area will increase. The algorithm is schematically depicted in Figure 5.

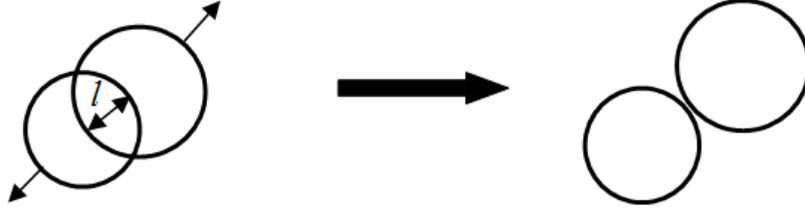The algorithm can be summarised as follows:

Figure 5: A schematic of the algorithm for calculating gravity-viscous spreading of an oil slick represented as a cloud of discs. The overlap is labelled l.

1. The radius of each disc i is calculated as

$$r_i = \sqrt{\frac{V_i}{\pi h_i}}$$

2. For each disc i the distances between the centre of that disc and the centres of each of the remaining discs $d_{c,j}$ are calculated and the overlap l_{ij} in each case is determined as

$$l_{ij} = r_i + r_j - d_{c,j}$$

3. The displacement of disc i in the horizontal due to overlapping with disc j (i.e. only when $l_{ij} > 0$) is then set to

$$\Delta x_{ij} = -0.5 \frac{(x_{c,j} - x_{c,i})}{d_{c,j}} l_{ij}$$

$$\Delta y_{ij} = -0.5 \frac{(y_{c,j} - y_{c,i})}{d_{c,j}} l_{ij}$$

where $(x_{c,i}, y_{c,i})$ is the position of the centre of disc i. This ensures that the displacements are in opposite directions along the axis between the centres of the discs and of the appropriate magnitude (see figure 5). If two discs are located right on top of each other, i.e. $d_{c,j} = 0$, then the direction of their displacements are set to random values.

4. The displacements for each disc relative all other discs are added together to produce the final displacement

$$(\Delta x_i, \, \Delta y_i) = \left(\sum \Delta x_{ij}, \, \sum \Delta y_{ij} \right) \tag{35}$$

with a magnitude given by

$$\Delta_i = \sqrt{(\Delta x_i)^2 + (\Delta y_i)^2}$$

This iterative spreading process is sensitive to the time step in relation to the size of the displacements. To ensure a smooth realistic spreading, the displacement magnitude for each disc is limited by a maximum displacement given by

$$\Delta_{i,\max} = \min\left(r_i, 0.5 \times \min\left(l_{ij}\right)\right)$$

If the displacement Δ_i is greater than $\Delta_{i,\max}$ then

$$\Delta x_i = \Delta x_i \frac{\Delta_{i,\max}}{\Delta_i}$$

and likewise for Δy_i.

4.4 Dispersion

Dispersion is defined as the process of spreading particles from the surface down into the water column. For dissolved substances this is simply modelled as turbulent mixing (see section 4.5 Mixing), but for oil a different approach is used.

Oil often forms cohesive slicks on the sea surface. Ordinary turbulent mixing generated by wind shear is unlikely to break up these slicks and disperse the resulting immiscible droplets into the water column. Instead, we assume that the mechanism of dispersion is the breaking of surface waves over the oil slick, breaking apart the slick and pushing down oil droplets to a depth dependent on the wave energy (see [7, 20]).

First, a number of droplet size classes are constructed, spanning a reasonable range (default is 20 classes ranging from 10^{-5} to 2×10^{-3}m in diameter). Next the dissipation breaking wave energy E_b is calculated from the breaking wave height H_b according to

$$E_b = 0.0034\rho g H_b^2 \tag{36}$$

The fraction of surface covered by breaking waves per unit time is estimated as

$$F_b = 3 \times 10^{-6} W^{3.5} \tag{37}$$

where W is the wind speed. We use the simple estimate $H_b = 1.5H_s$ to determine the breaking wave height from the significant wave height. The mass of oil to be dispersed for each size class Q_d is then calculated according to

$$Q_d = r_{ice}\Delta t c_\nu E_b^{0.57} F_b \overline{d}^{0.7} \Delta d A_{oil} \tag{38}$$

Here, r_{ice} is a correction factor to take into account the presence of ice, $c_\nu = 4450\nu_{oil}^{-0.4}$ is an empirical coefficient dependent on the oil viscosity in centistokes (cSt), $\overline{d}$ is the mean diameter for the current size class, Δd is the diameter interval of the size class and A_{oil} is the surface area of the oil slick. The ice correction factor is given by

$$r_{ice} = \begin{cases} 0 & C_{ice} \geq 0.8 \\ \frac{(0.8-C_{ice})}{0.5} & 0.3 \leq C_{ice} < 0.8 \\ 1 & C_{ice} < 0.3 \end{cases} \tag{39}$$

This means there is no dispersion for high ice concentrations, since it is assumed that the wave field is strongly damped by the ice.

Summing Q_d over all size classes we get a total mass to disperse. To determine which particles are to be dispersed, we randomly pick particles from all of those present on the surface and add up their resulting mass until we have reached the total mass to disperse. Each particle is assigned a diameter from the size class distribution based on the distribution of Q_d, beginning from the lower end of the distribution. Care is taken to ensure that the entire distribution is covered. Finally, each particle is assigned a depth to which it will be dispersed determined as a random value between zero and the intrusion depth $D_i = 1.5H_b$.

The dispersion is implemented by assigning each dispersed particle a large negative vertical velocity and continuing to calculate the particle's movement until the dispersion depth has been reached, after which the particle is assumed to represent a cloud of dispersed oil droplets of given diameter.

4.5   Mixing

This process is the result of small-scale isotropic turbulence in the fluid. The turbulence is usually modelled as a turbulent viscosity in hydrodynamic models, which must be interpreted in terms of turbulent contributions to the particle velocity. Turbulence is characterised by randomness and is an important factor in the vertical, though almost negligible on the larger, horizontal scales.

To calculate the turbulent velocities we use a Markov chain model (see [19]). From the turbulent kinetic energy k and its dissipation rate ε we can determine the turbulent eddies velocity scale and time scale, U' and T'. The Markov chain ensures that there is a memory, i.e. for short time steps the previously calculated turbulent velocity contributions exert a strong influence on the present values, whereas for long time steps there is no autocorrelation between successive instances of time.

In addition the model includes a third term to take into account the effect of a gradient in the turbulent intensity. This is to avoid the unphysical trapping of particles in areas of low turbulence.

The algorithm assumes that the time step is greater than the Taylor microscale (related to the smallest eddies where molecular processes become important) and smaller than the integral time scale of the turbulent motions. Violation of this condition will not cause the algorithm to fail, but the resulting dispersion will be too low if the time step exceeds the integral time scale. Common values for the integral time scale in a marine surface boundary layer are in the range 10 to 10^3 seconds.

The turbulent velocity contribution u' in a particular direction is calculated according to

$$u'(t) = Au'(t - \Delta t) + BPU' + C \tag{40}$$

Here,

$$A = e^{\frac{-\Delta t}{T'}} \tag{41}$$

$$B = \sqrt{1 - A^2} \tag{42}$$

$$C = 0.3T'(1 - A)\frac{\partial k}{\partial x} \tag{43}$$

P is a normally distributed random number in the interval [-1,1].

The equations are identical for the other two coordinate directions if one exchanges u' with v' or w' and x with y or z. The turbulent velocity scale is given by

$$U' = \sqrt{0.3k} \tag{44}$$

and the turbulent integral time scale by

$$T' = 0.3\frac{k}{\varepsilon} \tag{45}$$

The turbulent kinetic energy and its dissipation rate are calculated by the turbulence model in HIROMB and thus constitute input to PADM.

4.6 Buoyancy

Particles which do not have neutral buoyancy either sink or rise. The buoyancy velocity w_s is calculated assuming a piece-wise linearly varying vertical density stratification.

If the particles can be represented as spheres of given diameter d and density ρ_P, a formula primarily developed for oil (see [21]) is used which depends on the value of the critical diameter

$$
d_{crit} = \alpha \frac{\nu^{2/3}}{|g'|^{1/3}}
$$

where g' is the reduced gravity (buoyancy)

$$
g' = g \left(1 - \frac{\rho_P}{\rho} \right)
\tag{46}
$$

The buoyancy velocity is then calculated according to

$$
w_s = \begin{cases} \frac{g'}{|g'|} \sqrt{\beta d \, |g'|} & d > d_{crit} \\ \frac{g'}{|g'|} \left(\frac{d^2 |g'|}{18 \nu} \right) & d \leq d_{crit} \end{cases}
\tag{47}
$$

These two expressions represent the large, spherical-cap bubble regime and the small spherical droplet (Stokes's) regime discussed in [31]. The values of α and β are 9.52 and 8/3, respectively (see [21]). Note that α is given by equating the two expressions for w_s and solving for d. However, the value for β is probably too large (see [31]), producing a too high buoyancy velocity for large diameters. Hence, in PADM the value 0.711^2 proposed in [31] is used for β, yielding a value of 5.47 for α.

Alternatively another formula may be used, which is developed primarily for sand grains (see [23]). In [31] a new formulation is proposed that considers three regimes - small spherical droplets, intermediate ellipsoid bubbles and large spherical-cap bubbles - but this has yet to be implemented.

The droplet diameter for oil is determined by three processes:

1. For oil that has been dispersed from the surface the diameter is given by the droplet diameter calculated by the dispersion algorithm (see section 4.4).

2. For oil released at depth the droplet diameter is determined by random sampling from a given normal distribution, defined by its mean, its standard deviation and limited by a minimum value greater than zero. The

values of these three parameters are currently unknown and have been adjusted to fit available observations of the surface spreading of a single oil spill. The present values are 5 mm for the mean diameter, 2 mm for the standard deviation and 0.01 mm for the minimum droplet diameter.

3. For oil that is mixed down from the surface due to the action of turbulence the droplet diameter is set equal to the thickness of the surface spill.

In the case of substances other than oil, a representative particle diameter must be supplied at the start of the simulation.

If the particles cannot be represented as droplets or bubbles, or the relevant diameter is unknown, then the following simple model is used:

$$w_s = c_s g'$$ (48)

Here, c_s is an adjustable coefficient.

4.7 Boundary interaction

Boundaries in PADM can be of different categories: the sea surface, the coastline, the horizontal sea bed, the vertical sea bed and open boundaries.

For each boundary category a boundary action can be set. This determines what action should be taken when a particle's trajectory intersects a boundary. Three types of boundary actions are currently available in PADM: slip, halt and deactivation.

- *Slip* means that a particle cannot pass through a boundary but may move tangentially along it.

- *Halt* means that the particle is held at the location where it hit the boundary and its position is no longer updated, unless it is released again. However, other processes such as weathering may proceed to act on the particle.

- *Deactivation* means that the particle is completely frozen and no longer takes part in the calculations.

In the current implementation of Seatrack Web HELCOM different boundary actions have been set depending on the type of substance represented by the particles. For oils, the slip action is used for the sea surface but for all other boundaries deactivation occurs. This means that oil that intercepts the coastline or the bottom is assumed to stick in place and not undergo any more weathering. For other substances, e.g. floating objects, algae, etc., the slip action is used for all boundaries except open boundaries, where instead deactivation occurs.

5 Oil weathering

When Seatrack Web is used to forecast oil drift, each particle represents a quantity of oil with a common set of properties:

- mass and volume of oil plus water-in-oil,

- mass of oil,

- density of oil,

- mass of water-in-oil and

- bulk viscosity.

These properties are variables that change due to two different processes: evaporation and emulsification.

A number of different petroleum products can be simulated, ranging from the light and volatile gasoline and kerosene to asphalt.

There are currently two alternative weathering models in PADM: one based on a proprietary code supplied by SINTEF (e.g. [6]) and the original Seatrack Web model based on simple empirical formulae (see [11, 16]). Which model is used depends on the type of oil being simulated, as the empirical constants used in the two models have been determined for different sets of petroleum products.

5.1 The SINTEF model

This model is based on tables of empirical data for relevant oil properties which show how these properties change in time. Interpolation into these tables gives the values at a given point in time, and these values are then used to determine the evaporation, emulsification, density and viscosity.

5.1.1 Evaporation

The empirical data contains values of the evaporated fraction in percent f_e at different evaporation exposure times. The mass of oil M after a given time of exposure is then simply given by

$$M = (1 - f_e/100) \, M_0 \qquad (49)$$

Here, M_0 is the initial mass of fresh oil. The evaporation exposure time t_{evap} is however not only a function of time, but of several other factors as well. The increase in the exposure time is given by

$$\Delta t_{evap} = \frac{\Delta t}{3600} \left(1 - C_{ice}\right) \frac{W}{W_{ref}} \frac{h_{ref}}{1000 h} T_{corr} \qquad (50)$$

W_{ref} and h_{ref} are reference values for the wind speed and oil thickness, respectively, for which the property tables have been generated. Note that h_{ref} is defined in mm, hence the factor 1000, and t_{evap} is defined in hours. The temperature dependent correction factor is given by

$$T_{corr} = 2^{\frac{T - T_{ref}}{8}} \qquad (51)$$

Here, T is the sea surface temperature and T_{ref} a reference temperature for which the property tables have been generated. The maximum exposure time, i.e. when no more evaporation occurs and the oil is completely weathered, is set to 3360 hrs (140 days).

Evaporation is only calculated for oil on the surface. If the total mass of a particle reaches zero all the oil is assumed to have evaporated and the particle is deactivated.

5.1.2 Emulsification (water-in-oil)

The empirical data contains values of the mass fraction in percent of water in a water-in-oil emulsion m_w for different emulsification exposure times. The mass of water in a water-in-oil emulsion M_w is then calculated as

$$M_w = M \frac{m_w}{100 - m_w} \qquad (52)$$

The emulsification exposure time t_{emul} is again not only a function of the time (see section 5.1.1), but is calculated using the following expression for the increase in exposure time:

$$\Delta t_{emul} = \frac{\Delta t}{3600} \frac{\left(\left(1 - C_{ice}\right) W + 1\right)^2}{\left(W_{ref} + 1\right)^2} \qquad (53)$$

It is assumed that dispersed oil droplets do not form a water-in-oil emulsion. Thus, if oil that has formed a water-in-oil emulsion is dispersed, all the water is immediately removed.

5.1.3 Density

The empirical data contains values of the density of oil ρ_{oil} at different evaporation exposure times (see section 5.1.1). The particle density including the effect of emulsification ρ_P is calculated according to

$$\rho_P = \frac{1}{\frac{(1-m_w)}{\rho_{oil}} + \frac{m_w}{\rho}} \tag{54}$$

where the water mass fraction is determined from

$$m_w = \frac{M_w}{M_w + M} \tag{55}$$

5.1.4   Viscosity

The empirical data contains values of the oil viscosity μ_{oil} in cP at different evaporation exposure times (see section 5.1.1) as well as the viscosity of a stable water-in-oil emulsion μ_{emul} in cP at different emulsification exposure times (see section 5.1.2). First, the viscosity considering only evaporation is determined by interpolation into the table of empirical data on μ_{oil} and then adjusted for the actual sea water temperature T according to

$$\mu_{oil}(T) = 10^{10^{\lambda}} \tag{56}$$

$$\lambda = -0.0045\,(T - T_{ref}) + \log\left(\log\left(\mu_{oil}\right)\right) \tag{57}$$

Here, T_{ref} is the reference temperature for which the property tables have been generated (see section 5.1.1). The particle viscosity including the effect of emulsification μ_P is then determined according to

$$\mu_P = F_{emul}\mu_{oil}(T) \tag{58}$$

where the ratio between the viscosities of water-in-oil emulsion and oil F_{emul} is determined by interpolating into a new table, generated by dividing the empirical data on μ_{emul} by the data on μ_{oil}, at the current emulsification exposure time. The particle viscosity is then converted to kinematic particle viscosity (unit cSt) according to

$$\nu_P = \frac{\mu_P}{0.001\rho_P} \tag{59}$$

5.2   The original Seatrack Web model

All oils are represented using a two-component model, i.e. they consist of a volatile and a non-volatile component. The oil properties are defined in a database file and comprise the following set of parameters:

- densities of the volatile and non-volatile components,

- viscosity,

- the maximum water fraction of emulsified oil,

- the level of evaporation required for emulsification to begin,

- an emulsification rate coefficient,

- the fraction of the oil which is non-volatile,

- two rate coefficients for evaporation and

- three coefficients for calculating the viscosity.

The densities and the viscosity are approximate standard values for fresh oils at typical sea water temperatures.

At the beginning of a simulation oils are considered either fresh or completely weathered.

5.2.1 Evaporation

Evaporation is calculated based on simple expressions for the evaporation of the form (see [11, 16])

$$f_e = (C_1 + C_2 T) \ln \left(\frac{t}{60} \right) \tag{60}$$

Here, f_e is the percentage fraction of the particle mass that has evaporated, C_1 and C_2 are coefficients, T is temperature (°C) and t is time (s). Values for C_1 and C_2 for different oils are presented in [16]. A very minor modification to equation 60 removes the singularity at $t = 0$:

$$f_e = (C_1 + C_2 T) \ln \left(\frac{t}{60} + 1 \right) \tag{61}$$

This expression is a solution to

$$\frac{df_e}{dt} = \frac{(C_1 + C_2 T)}{60} e^{-f_e/(C_1 + C_2 T)} \tag{62}$$

Here we will derive a similar equation for the evaporation used in PADM. Assuming a two-component model, the oil mass M is given by

$$M = M_v + M_n \tag{63}$$

Subscript v denotes the volatile component and subscript n the non-volatile component. Only the volatile component evaporates, and thus the non-volatile mass is constant, i.e.

$$M_n = M_{n,0} \tag{64}$$

Henceforth, subscript 0 denotes the values at $t = t_0$, i.e. for fresh oil. The maximum fraction that can evaporate

$$E_{\max} = \frac{M_{v,0}}{M_0} \tag{65}$$

and the fraction of the total oil mass that is non-volatile

$$\frac{M_n}{M_0} = 1 - E_{\max} \tag{66}$$

are oil-specific constants. Further,

$$E = \frac{(M_{v,0} - M_v)}{M_0} = E_{\max} - \frac{M_v}{M_0} \tag{67}$$

is the fraction evaporated and thus

$$M_v = M_0 \left(E_{\max} - E \right) \tag{68}$$

If we model the fractional evaporation rate as

$$\frac{dE}{dt} = C_e e^{-\frac{K}{C_e} E} \tag{69}$$

where C_e and K are coefficients of dimension $1/t$, the solution is

$$E = \frac{C_e}{K} \ln \left(e^{\frac{K}{C_e} E_0} + K \left(t - t_0 \right) \right) \tag{70}$$

Here, $E_0 = E(t_0)$. We can thus calculate E at time t as a function of temperature and the value at time t_0. With $100E = f_e$ we can identify the coefficients using equation 62 as

$$K = \frac{1}{60} \tag{71}$$

and

$$C_e = \frac{K}{100} \left(C_1 + C_2 T \right) \tag{72}$$

To account for the presence of ice, the equation for dE/dt is modified such that

$$\frac{dE}{dt} = r_{ice} C_e e^{-\frac{K}{C_e E}} \tag{73}$$

Here, r_{ice} is a reduction factor given by equation 39. The equation for E then becomes

$$E = \frac{C_e}{K} \ln \left(e^{\frac{K}{C_e} E_0} + K r_{ice} \left(t - t_0 \right) \right) \tag{74}$$

Finally, using equation 68 the new oil mass is calculated according to

$$M = M_v + M_n = M_0 \left(E_{\max} - E + m_n \right) \tag{75}$$

Evaporation is only calculated for oil on the surface. If the total mass of a particle reaches zero all the oil is assumed to have evaporated and the particle is deactivated.

5.2.2   Emulsification (water-in-oil)

Emulsification is a process by which water is incorporated into the oil, forming a highly viscous emulsion or mousse. Here, we assume that only oil on the surface will emulsify. Furthermore, the oil will not emulsify until a certain fraction E_{emul} of the volatile components has evaporated.

The rate at which the oil forms an emulsion is related to the wind speed W, as the process requires agitation of oil and water. Thus, the emulsion rate R is modelled by

$$R = \begin{cases} 0, & E < E_{emul} \\ r_{ice} C_R W^2, & E \geq E_{emul} \end{cases} \tag{76}$$

Here, r_{ice} is the same reduction factor as for evaporation (see equation 39) to account for the presence of ice and C_R is an oil-specific constant coefficient.

The mass fraction of water in a water-in-oil emulsion m_w is defined by

$$m_w = \min \left(m_{w,\max}, \frac{M_w}{M_w + M} \right) \tag{77}$$

Here, $m_{w,\text{max}}$ is an oil-specific maximum water fraction for water-in-oil emulsion and M_w is the mass of water in the water-in-oil emulsion. The rate of change of m_w is [17]

$$\frac{dm_w}{dt} = R\left(m_{w,\text{max}} - m_w\right) \tag{78}$$

Integrating this equation yields

$$m_w\left[t\right] = m_{w,\text{max}} - e^{-R(t-t_0)}\left(m_{w,\text{max}} - m_w\left[t_0\right]\right) \tag{79}$$

Setting $\Delta t = t - t_0 = t_{i+1} - t_i$ yields

$$m_w\left[t_{i+1}\right] = m_{w,\text{max}} - e^{-R\Delta t}\left(m_{w,\text{max}} - m_w\left[t_i\right]\right) \tag{80}$$

The mass of water in the emulsion is calculated from equation 77 as

$$M_w = M\,\frac{m_w}{1 - m_w} \tag{81}$$

It is assumed that dispersed oil droplets do not form a water-in-oil emulsion. Thus, if oil that has formed a water-in-oil emulsion is dispersed, all the water is immediately removed.

5.2.3 Density

The oil density is calculated from a simple two-component model according to

$$\rho_{oil} = \frac{1}{m_n/\rho_n + m_v/\rho_v} \tag{82}$$

Here, m_n and m_v are the mass fractions and ρ_n and ρ_v are the densities of the non-volatile and volatile oil components. The particle density ρ_P including the effect of emulsification is then calculated as

$$\rho_P = \frac{1}{\left(\frac{(1-m_w)}{\rho_{oil}} + \frac{m_w}{\rho}\right)} \tag{83}$$

5.2.4 Viscosity

The particle viscosity in cSt, including the effect of emulsification, is determined from the amount of the volatile fraction that has evaporated (E) and the degree of emulsification (fraction of water-in-oil) according to

$$\nu_P = \nu_{ref} e^{aE} e^{\frac{bm_w}{1-cm_w}} \tag{84}$$

Here, ν_{ref} is the reference oil viscosity (cSt) given in the oil properties database file whereas a, b and c are constant coefficients specific for each oil (see [17]).

6 Additional features

6.1 Uncertainty spreading

To provide an idea of the uncertainty in a drift simulation, it is possible to activate a feature called uncertainty spreading. In this case each particle is given an additional random velocity whose magnitude is a function of the expected uncertainty in the wind forecast. The idea is to mimic an ensemble of simulations with slightly different forcing. Only particles on the surface are affected.

The random velocity contribution to each particle is calculated according to

$$u'' = \sigma P \cos(2\pi Q) \tag{85}$$

$$v'' = \sigma P \sin(2\pi Q) \tag{86}$$

$$w'' = 0 \tag{87}$$

Here, P is a random number from the normal distribution and Q a random number from the uniform distribution. Both are assigned once at the beginning of the simulation and then kept constant, though a different value for each particle. The parameter σ is given by the standard deviation of the error in the forecasted wind speed σ_W multiplied by a factor to produce a resulting variability in the wind-driven surface current:

$$\sigma = 0.02\sigma_W \tag{88}$$

It is assumed that the error in the wind forecast is normally distributed. Thus, $\sigma_W = {}^{\Delta w}\!/_{1.44}$ where Δ_W is an estimate of the absolute error of the wind speed forecasted by the meteorological model HIRLAM, and which covers 85 % of observed wind speeds [14]:

$$\Delta_W = \begin{cases} 2.0 & W < 2.0 \\ 1.7 + 0.195W & W \geq 2.0 \end{cases} \tag{89}$$

References

[1] Anderson, E., 2001: "Oil in Ice Modelling: OILMAP Implementation", ASA Report, Project No. ASA 00-149, Applied Science Associates, Inc., USA, pp 13.

[2] ARCOP, 2004: "State of the art report on oil weathering and on the effectiveness of response alternatives", Report 4.2.1.1(a), July 2004 (`http://www.arcop.fi/reports.htm`).

[3] ARCOP, 2005: "Simulations of oil drift and spreading and oil spill response analysis", Report 4.2.2.2/4.2.2.3, June 2005 (`http://www.arcop.fi/reports.htm`)

[4] Banner, M.L., 1990: "Equilibrium Spectra of Wind Waves", Journal of Physical Oceanography, 20, pp. 966-984.

[5] Comfort, G., 1987: "Analytical modelling of oil and gas spreading under ice", Environmental Studies Research Fund, Report No. 077, Aug., Arctec Canada Limited, 16, 6325, 11 Street, S.E., Calgary, Alberta, Canada, pp. 57.

[6] Daling, P.S., and Strøm, T., 1999: "Weathering of oil at sea; model/field data comparisons", Spill Science and Technology Bulletin 5 (1), 63–74.

[7] Delvigne, G., and Sweeney, C., 1988: "Natural dispersion of oil", Oil & Chemical Pollution, 4, 281-310.

[8] Dickins, D. F., 1992: "Behaviour of oil spilled at sea (BOSS): oil-in-ice fate and behaviour", DF Dickins Associates and Fleet Technology Ltd. For Environment Canada, March 1992 (`http://www.mms.gov/tarprojects/120/120AT.pdf`).

[9] Dickins, D.F., and Buist, I., 1999: "Countermeasures for ice covered waters", Pure Appl. Chem. Vol 71, No 1, pp. 173-191 (`http://www.iupac.org/publications/pac/special/0199/pdfs/dickins.pdf`).

[10] Donelan, M.A., J. Hamilton and W.H. Hui, 1985: "Directional spectra of wind generated waves", Phil. Trans. Roy. Soc. London, A315, pp. 509-562.

[11] Fingas, M.F., 1999: "The Evaporation of Oil Spills: Development and Implementation of New Prediction Methodology", in: Proceedings of The 1999 International Oil Spill Conference, American Petroleum Institute, Washington, D.C., pp. 281-287.

[12] Fingas, M. F., and Hollebone, B. P., 2003: "Review of behaviour of oil in freezing environments", Marine Pollution Bulletin, 47, (9-12), pp. 333-340.

[13] Hasselmann, K., et al, 1973: "Measurements of wind growth and swell during the Joint North Sea Wave Project (JONSWAP)", Deutsche Hydrographische Zeitschrift, suppl. A, 8, 12.

[14] Häggmark, L. (pers. comm.)

[15] Kahma, K.K. and C.J. Calkoen, 1992: "Reconciling discrepancies in the observed growth of wind-generated waves", Journal of Physical Oceanography, 22, pp. 1389-1405.

[16] Lindgren, C. et al, 2001: "Seatrack Web - algoritmer för vädringsprocesser på oljor ute till havs", IVL Svenska Miljöinstitutet AB, report for the Swedish Coast Guard and the Swedish Rescue Services Agency, September 2001 (in Swedish).

[17] Lehr, W. J., 2001: "Review of modelling procedures for oil spill weathering behaviour", In: Oil Spill Modelling and Processes, (Brebbia, C.A., ed), WIT Press, Southampton, UK, pp. 51-90.

[18] Liu, S., and Leendertse, J. J., 1981: "A 3-D Oil Spill Model With and Without Ice Cover", International Symposium on Mechanics of Oil Slicks, September 8, Paris, France, pp 23.

[19] Rahm, L.-A., and Svensson, U., 1986: "Dispersion of marked fluid elements in a turbulent Ekman layer". J. Phys. Oceanogr., 16, 2084-2096.

[20] Reed, M., French, D., Rines, H., and Rye, H., 1995: "A three-dimensional oil and chemical spill model for environmental impact assessment", 1995 Oil Spill Conference, 61-66.

[21] Soares dos Santos, A., and Daniel, P., 2000: "Oil spill modelling near the Portuguese coast", In: Oil & Hydrocarbon Spills II, Eds. G.R. Rodriguez & C.A. Brebbia, WIT Press, p. 11-18.

[22] SINTEF, 2003: "Oil Weathering Model User's Manual Version 3.0" (http://www.mms.gov/alaska/reports/2005rpts/2005_020/Final%20Report/Appendix%20D/User%20Manual%20for%20SINTEF%20Oil%20Weathering%20Model%203_0.pdf).

[23] Soulsby, R., 1997: "Dynamics of marine sands", HR Wallingford Ltd., p. 134.

[24] Venkatesh, S., El-Tahan, H., Comfort, G., and Abdelnour, R., 1990: "Modelling the behaviour of oil spills in ice-infested waters", Atmosphere Ocean 28 (3), pp. 303-329.

[25] Welsh, J. P., Lissauer, I. M., Hufford, G. L., Ellis, T. S., Thompson, B. D., Farmer, L. D., and Hiltabrand, R. R., 1977: "Some dynamics of spilled oil in a fractured ice field in Buzzards Bay", Massachusetts Ocean Engineering, Vol 4, (4-5), pp. 197-203.

[26] Wolk, F., 2003: "Three-dimensional Lagrangian tracer modelling in Wadden Sea areas", Diploma thesis, Carl von Ossietzky University Oldenburg, Hamburg.

[27] Yapa, P. D., and Chowdhury, T., 1990: "Spreading of oil under ice", Journal of Hydraulic Engineering, 116, (12), pp. 1468-1483.

[28] Yapa, P. D., Weerasuriya, S. A., Belaskas, D. P., and Chowdhury, T., 1993: "Oil spreading in surface water with an ice cover", Report 93-3, Civil and Environmental Engineering, Clarkson University, Potsdam, NY, USA.

[29] Yapa, P. D., Weerasuriya, S. A., 1997: "Spreading of oil spilled under floating broken ice", Journal of Hydraulic Engineering – ASCE, 123, (8), pp. 676-683.

[30] Young, I., 1999: "Wind generated ocean waves", Elsevier.

[31] Zheng, L. & Yapa, P. D., 2000: "Buoyant velocity of spherical and nonspherical bubbles/droplets", J. of Hydraulic Engineering, November, pp. 852-854.